

KAgF₃: quasi-one-dimensional magnetism in three-dimensional magnetic ions sublattice

Xiaoli Zhang, Guoren Zhang, Ting Jia, Ying Guo, and Zhi Zeng*

Key Laboratory of Materials Physics, Institute of Solid State Physics,

Chinese Academy of Sciences, Hefei 230031, P. R. China

H. Q. Lin

Department of Physics and Institute of Theoretical Physics,

The Chinese University of Hong Kong, Shatin, Hong Kong, P. R. China

(Dated: March 8, 2019)

The ground-state electronic structure and magnetic properties of the Jahn-Teller-distorted perovskite KAgF₃ have been investigated using the full-potential linearized augmented plane-wave method. It is found that KAgF₃ exhibits significant quasi-one-dimensional antiferromagnetic characteristics with the ratio of exchange constant J_{\perp} (perpendicular to the b axis) and J (along the b axis) about 0.04, although the sublattice of magnetic ions is three-dimensional. The strong spacial exchange anisotropy originates from the hole-orbital ordering of the Ag²⁺ $4d^9$ ions. The orbital ordering could be stabilized when the structure distortions are taken into account in isolation. Moreover, the on-site Coulomb repulsion is crucial for opening an insulating gap in KAgF₃, as confirmed by the present total energy calculations.

PACS numbers: 75.25.-j, 71.20.-b

* Correspondence author. Email: zzeng@theory.issp.ac.cn

I. INTRODUCTION

Low-dimensional magnets have attracted many researchers because of their unique electronic and magnetic properties. For example, the physical properties of quasi-2D high-temperature superconductor^{1,2}, spin-Peierls compound³, Haldane chain⁴ and spin-ladder⁵ as well as spin-frustrated^{6,7} systems have been extensively investigated. In most of the low-dimensional magnets, the magnetic cation sublattices consist of planes or chains which are kept reasonably far apart. However, materials which exhibit one-dimensional (1D) magnetic behavior within three-dimensional (3D) magnetic ions sublattice are rare. KCuF_3 is one of these materials possessing both a 3D sublattice and effectively 1D magnetic properties.^{8,9} Up to date, the electronic orbital ordering (OO) is considered as an essential factor in stabilizing the abnormal magnetic structure in KCuF_3 .^{10,11}

KAgF_3 is a structural analog of KCuF_3 . Its crystal structure is pseudocubic and is made up of an array of John-Teller (JT) type AgF_6 octahedra.¹² The JT distortion divides the Ag-F bonds in each octahedron into long, intermediate and short ones. The long and short Ag-F bonds are aligned alternatively in the ac plane. The intermediate Ag-F bonds form AgF zig-zag chains along the b axis. It is obvious that the distances of nearest magnetic ions are nearly the same in all three principal axes in Ag ions sublattice. Moreover, similar to KCuF_3 , KAgF_3 also has $S=1/2$ divalent transition-metal cations ($\text{Ag}^{2+} 4d^9$ vs $\text{Cu}^{2+} 3d^9$). Therefore, we expect KAgF_3 has the similar properties of KCuF_3 . That is, it should exhibit quasi-one-dimensional magnetism within a three-dimensional magnetic ions sublattice. To the best of our knowledge, there are possibly no theoretical reports yet, therefore we expect to understand the magnetic properties of KAgF_3 upon our theoretical efforts.

In the present work, we investigate the electronic structure and the magnetic properties of KAgF_3 by density functional theory (DFT) total energy calculations. The calculated $J_{\perp}/|J|=0.04$ indicates that the compound is an quasi-1D antiferromagnet. Here, J (J_{\perp}) refers to exchange constant along (perpendicular to) the b axis. The inherent lattice distortion is accompanied by the Ag $4d$ hole OO, and this OO accounts for the abnormal antiferromagnetism in KAgF_3 . The on-site Coulomb repulsion is crucial for opening an insulating gap in KAgF_3 .

II. CALCULATION METHODS

Our electronic structure calculations are performed within the full-potential linearized augmented plane-wave framework.¹³ In the calculation the generalized gradient approximation (GGA) of Perdew-Burke-Ernzerhof form is adopted.¹⁴ To include the on site Coulomb interaction GGA+ U (U =on-site Coulomb repulsion strength) approach are carried out. The on-site Coulomb repulsion U is handled with the self-interaction corrected method proposed by Anisimov and co-workers, in which the $U_{eff}=U-J$ (J is the exchange interaction) was used instead of U .^{15,20} Here in our work, on-site Coulomb repulsion U is applied to Ag $4d$ orbitals only. The muffin-tin sphere radii are chosen to be 2.46, 2.09, and 1.85 bohr for K, Ag, and F atoms, respectively. The value of $R_{MT}K_{max}$ (the smallest muffin-tin radius multiplied by the maximum k value in the expansion of plane waves in the basis set) is set to 7.0. We use 500 k points (i.e., 196 k points in the irreducible wedge of the Brillouin zone) for the integration over the Brillouin zone of the primitive cell with the experimental lattice constants $a=6.2689$ Å, $b=8.3015$ Å, and $c=6.1844$ Å.¹²

Experimentally, $KAgF_3$ undergoes a metal-insulator transition coincident with an anti-ferromagnetic (AFM) ordering temperature.¹⁸ In order to determine the spin arrangements, we carried out total energy calculations with three distinct spin configurations as described in Fig. 1. These spin configurations were (1) ferromagnetic (FM), (2) A -type AFM (ferromagnetism in ac plane, AFM stacking), and (3) G -type AFM (antiferromagnetism in ac plane, AFM stacking).

III. RESULTS AND DISCUSSIONS

Fig. 2 shows the total and partial density of states (DOS) for the lowest energy spin configuration of A -type AFM $KAgF_3$ within GGA. The predominance of Ag $4d$ and F $2p$ states between -7 eV and the Fermi level implies hybridization between these states. The strong Ag $4d$ -F $2p$ hybridization in this compound can be understood in terms of the extended nature of Ag $4d$ electrons. The partial DOS of apical F (F_{ap}) is more extended than that of planar F (F_{pl}), indicating the hybridization between the Ag $4d$ and the F_{ap} is stronger than the hybridization between the Ag $4d$ and the F_{pl} . Such difference is caused by OO which will be discussed later in this paper.

However, GGA approach could not capture the insulating behavior of KAgF_3 , as shown in Fig. 2. It is well known that such *ab initio* calculations often underestimate the on-site Coulomb correlation effect, which plays significant role in determining the electronic properties of d and f electron systems.¹⁷ Thus, we carry out GGA+ U calculations with different values of U . It is insulating for all the FM, A -type AFM and G -type AFM spin configurations independent of U (4-7 eV). Actually, even the calculations with $U=1$ eV already give an insulating solution with an energy gap of about 0.03 eV for A -type AFM ground state, implying the Ag $4d$ -electron correlation is moderate. The energy gap increases considerably up to 2.22 eV for $U=7$ eV, since the electron-electron repulsion pushes up the unoccupied states in energy. The remarkable increase in the gap value is accompanied by the enhancement of the spin magnetic moment from $\pm 0.41\mu_B/\text{Ag}$ to $\pm 0.68\mu_B/\text{Ag}$ as U is increased from 1 to 7 eV. Because the opening up of an insulating gap requires on-site Coulomb interaction among Ag $4d$ electrons, we focus our discussion on the GGA+ U case with $U=4$ eV in the following. Such a value of U was used in another Ag^{2+} compound Cs_2AgF_4 and reasonable results were obtained.¹⁹

Fig. 3 shows the total and partial DOS for A -type AFM state of KAgF_3 within GGA+ U (4 eV). The Coulomb repulsion U pushes the occupied $4d$ levels downward. As a result, the lower-lying bonding states have a larger Ag $4d$ characteristic than the higher-lying antibonding states, in contrast to the GGA results shown in Fig. 2. Although GGA+ U tends to enhance the localization of Ag $4d$ states, Ag $4d$ states are more extended compared with the $3d$ states. Due to the strong Ag-F covalency, the one hole state of Ag $4d^9$ spreads, over the six fluorine atoms of the AgF_6 octahedron. This is also reflected by the smaller Ag ($\pm 0.53\mu_B$) and non-zero F_{pl} ($\pm 0.1\mu_B$) spin magnetic moments within each muffin-tin sphere. The magnetic moment obviously vanishes for F_{ap} atoms contained within AgF chains (due to symmetry), as shown in table I.

As shown in table I, A -type AFM is only 15 meV lower in energy than the G -type AFM, and both A -type AFM and G -type AFM are much lower in energy than FM spin configuration. This suggests a quasi-one-dimensional magnetic behavior of KAgF_3 : The magnetic interaction along y' direction is much stronger than that in the $x'z'$ plane. To gain additional insight into the quasi-one-dimensional magnetic behavior of KAgF_3 , we have evaluated the magnetic exchange constants along and perpendicular to the b axis numerically

in terms of the Heisenberg spin Hamiltonian:

$$H = J \sum_{i,j} \mathbf{S}_i \cdot \mathbf{S}_j + J_{\perp} \sum_{k,l} \mathbf{S}_k \cdot \mathbf{S}_l \quad (1)$$

where the first (second) term refers to summing over all nearest neighbors along (perpendicular to) the b axis. By mapping the obtained total energies for each magnetic state to the next nearest Heisenberg model, the exchange interactions J and J_{\perp} are

$$J = \frac{1}{8S^2} (E_{FM} - E_{A-type}) \quad (2)$$

$$J_{\perp} = \frac{1}{16S^2} (E_{A-type} - E_{G-type}) \quad (3)$$

With the spin $S=1/2$ of a $4d^9$ Ag^{2+} ion, we get $J=83.8$ meV and $J_{\perp}=-3.7$ meV, which reflects strong spatial exchange anisotropy. Note that J_{\perp} is negative and $|J_{\perp}|/J=0.04$, indicating strong 1D AFM coupling along the b axis and a much weaker FM coupling perpendicular to this axis. Thus, KAgF_3 is another material exhibiting 1D magnetic behavior within 3D magnetic ions sublattice. To our knowledge, there is no experimental evidence of spatial exchange anisotropy of KAgF_3 . For this reason, the neutron diffraction study of spin waves, which can give information about the spatial exchange anisotropy, would be very interesting topic for future experimental investigation.

The quasi-one-dimensional magnetic behavior within a 3D magnetic ions sublattice in KAgF_3 is associated with the formation of the OO. In KAgF_3 , the octahedral symmetry is broken by an electron orbital polarization accompanied by a cooperative JT distortion. Orbital polarization is obvious in the Ag1 $4d$ -resolved DOS in Fig. 4. The two-fold degenerate e_g bands are lifted and the one hole occupy the higher energy $x'^2-y'^2$ orbital. In addition, the cooperative JT distortion lead to alternating short and long Ag-F bonds in the $x'z'$ plane. Hence connecting the four shorter Ag-F bonds creates a plaquette in the $x'y'$ plane for one Ag1 site and in the $z'y'$ plane for one Ag2 site. The Ag1 $x'^2-y'^2$ hole state and Ag2 $z'^2-y'^2$ hole state form the C -type AFM hole OO (antiferro-distortive in the ab plane, ferro-distortive stacking), which is schematically shown in Fig. 5. Accordingly, our GGA+ U (4 eV) calculations have demonstrated the same C -type AFM hole OO in KAgF_3 as that in KCuF_3 .¹⁰ The C -type AFM hole OO gives rise to a strong superexchange interaction J between nearest neighbor Ag ions along the y' axis but small exchange interaction J_{\perp} in the $x'z'$ plane, because of the strong Ag1 $4d_{x'^2-y'^2}$ -F $2p$ -Ag1 $4d_{x'^2-y'^2}$ or Ag2 $4d_{z'^2-y'^2}$ -F

$2p$ -Ag $2 4d_{z^2-y'^2}$ and the weak Ag $1 4d_{x'^2-y'^2}$ -F $2p$ -Ag $2 4d_{z^2-y'^2}$ orbital overlap even though the distances between nearest neighbor ions are almost the same along all principal axes in magnetic Ag ions sublattice. The C -type AFM hole OO leads to the most stable A -type AFM state, in accord with the Goodenough-Kanamori rules. Our GGA+ U (4eV) calculations confirm this in view of that A -type AFM state being the most stable state. And the results of OO and the A -type AFM ground state are independent of the value of U .

As the discussion above, both of the KAgF_3 and KCuF_3 have the same C -type AFM hole OO, however, their mechanisms of OO are different. It is found that a electronically driven orbital polarization was observed even in the undistorted phase itself in KCuF_3 .²⁰ Our GGA calculation for A -type AFM ground state KAgF_3 , not including correlation effects, already gives an C -type AFM hole OO as shown in Fig. 6. Therefore, the orbitally ordered hole state in KAgF_3 is associated with the large distortion of the Ag-F bonds of 0.31 Å. Moreover, considering the on-site Coulomb repulsion without the JT distortion, we find that the GGA+ U ($U=5-7$ eV) calculations can not give any OO solution (not shown). Altogether, the dominant mechanism responsible for OO in KAgF_3 is the JT distortion, in strong contrast to the electronically driven orbital polarization in KCuF_3 .

IV. CONCLUSIONS

By means of GGA and GGA+ U band structure calculations, we have found that the perovskite KAgF_3 is one of very few materials to possess both a pseudocubic magnetic Ag ions sublattice and quasi-one-dimensional magnetic characteristic. The spatial exchange anisotropy is associated with the orbital ordering (OO). The OO could be stabilized when the structure distortions are taken into account in isolation. Moreover, the on-site Coulomb repulsion is crucial for opening an insulating gap in KAgF_3 . The quasi-one-dimensional magnetic property is still a theoretical prediction, and direct measurement of the spatial exchange anisotropy would be highly desirable.

V. ACKNOWLEDGMENTS

This work was supported by the special Funds for Major State Basic Research Project of China(973) under Grant No. 2007CB925004, 863 Project, Knowledge Innovation Program

of Chinese Academy of Sciences under Grant No. KJCX2-YW-W07, Director Grants of CASHIPS, and CUHK Direct Grant No. 2160345. Part of the calculations were performed in Center for Computational Science of CASHIPS and the Shanghai Supercomputer Center.

- ¹ G. Shirane, Y. Endoh, R. Birgeneau, M. Kastner, Y. Hidaka, M. Oda, M. Suzuki, and T. Murakami, *Phys. Rev. Lett.* **59**, 1613 (1987).
- ² Y. Kamihara, T. Watanabe, M. Hirano and H. Hosono, *J. Am. Chem. Soc.* **130**, 3296 (2008).
- ³ M. Shaz, S. van Smaalen, L. Palatinus, M. Hoinkis, M. Klemm, S. Horn, and R. Claessen, *Phys. Rev. B* **71**, 100405(R) (2005).
- ⁴ H. Tsunetsugu and Y. Motome, *Phys. Rev. B* **68**, 060405(R) (2003).
- ⁵ O. Pieper, B. Lake, A. Daoud-Aladine, M. Reehuis, K. Prokes, B. Klemke, K. Kiefer, J. Q. Yan, A. Niazi, D. C. Johnston, and A. Honecker, *Phys. Rev. B* **79**, 180409(R) (2009).
- ⁶ H. Kageyama, K. Yoshimura, K. Kosuge, H. Mitamura, and T. Goto, *J. Phys. Soc. Jpn.* **66**, 1607 (1997).
- ⁷ S. K. Pandey and Kalobaran Maiti, *Phys. Rev. B* **78**, 045120 (2008).
- ⁸ S. K. Satija, J. D. Axe, G. Shirane, H. Yoshizawa, and K. Hirakawa, *Phys. Rev. B* **21**, 2001 (1980).
- ⁹ K. I. Kugel and D. I. Khomskii, *Sov. Phys. Usp.* **25**, 231 (1982).
- ¹⁰ M. D. Towler, R. Dovesi, and V. R. Saunders, *Phys. Rev. B* **52**, 10150 (1995).
- ¹¹ E. Pavarini, E. Koch, and A. I. Lichtenstein, *Phys. Rev. Lett.* **101**, 266405 (2008).
- ¹² Z. Mazej, E. Goreshnik, Z. Jaglicic, B. Gawel, W. Lasocha, D. Grzybowska, T. Jaron, D. Kurzydowski, P. Malinowski, W. Kozminski, J. Szydlowska, P. Leszczynski and W. Grochala, *CrystEngComm* **11**, 1702 (2009).
- ¹³ P. Blaha, K. Schwarz, G. Madsen, D. Kvasnicka, and J. Luitz, <http://www.wien2k.at>
- ¹⁴ J. P. Perdew, K. Burke, and M. Ernzerhof, *Phys. Rev. Lett.* **77**, 3865 (1996).
- ¹⁵ V. I. Anisimov, I. V. Solovyev, M. A. Korotin, M. T. Czyzyk, and G. A. Sawatzky, *Phys. Rev. B* **48**, 16929 (1993).
- ¹⁶ A. I. Liechtenstein, V. I. Anisimov, and J. Zaanen, *Phys. Rev. B* **52**, R5467 (1995).
- ¹⁷ V. I. Anisimov, F. Aryasetiawan, and A. I. Lichtenstein, *J. Phys.: Condens. Matter* **9**, 767 (1997).

- ¹⁸ W. Grochala and P. P. Edwards, *Phys. Status Solidi B* **240**, R11 (2003).
- ¹⁹ H. Wu and D. I. Khomskii, *Phys. Rev. B* **76**, 155115 (2007).
- ²⁰ A. I. Liechtenstein, V. I. Anisimov, and J. Zaanen, *Phys. Rev. B* **52**, R5467 (1995).

FIG. 1: Schematic representation of three spin configurations used in our calculations. Only Ag atoms are drawn. The arrows indicate the direction of the spins in the ordered phase. Filled and open circles indicate two inequivalent Ag1 and Ag2 atoms. J (J_{\perp}) denotes the nearest exchange constant along y' (x' and z').

FIG. 2: (color online). The total and partial DOS of KAgF_3 for A -type AFM spin configuration from GGA. Solid black and short dot red lines indicate spin-up and spin-down states respectively.

FIG. 3: (color online). The total and partial DOS of KAgF_3 for A -type AFM spin configuration from GGA+ U with $U=4$ eV. Solid black and short dot red lines indicate spin-up and spin-down states respectively.

FIG. 4: (color online). The Ag $4d$ -resolved DOS of KAgF_3 in the A -type AFM spin configuration from GGA+ U with $U=4$ eV. Solid black and short dot red lines indicate spin-up and spin-down states respectively.

FIG. 5: (color online). The C -type hole orbital ordering is schematically shown.

FIG. 6: (color online). The contour plot (0.05 - 0.9 $e/\text{\AA}^3$) of spin density in $x'z'$ (Fig. 6(a)), $x'y'$ (Fig. 6(b)) and $z'y'$ (Fig. 6(c)) planes through the AgF_6 octahedra of KAgF_3 for A -type AFM state from GGA. The solid (dot) lines depict the spin-up(spin-down) states.

TABLE I: Electronic structure of KAgF_3 in FM, A -type AFM and G -type AFM spin configurations calculated by GGA+ U with $U=4$ eV. The total energy difference (ΔE , meV/f.u.), local spin moment ($/\mu_B$) of each Ag, apical F (F_{ap}), and planar F (F_{pl}) atoms are shown.

	ΔE	E_g	μ_B/Ag	μ_B/F_{ap}	μ_B/F_{pl}
FM	168	0.02	0.65	0.13	0.11
A -type AFM	0	1.05	± 0.58	0.00	± 0.10
G -type AFM	15	0.90	± 0.55	0.00	± 0.09

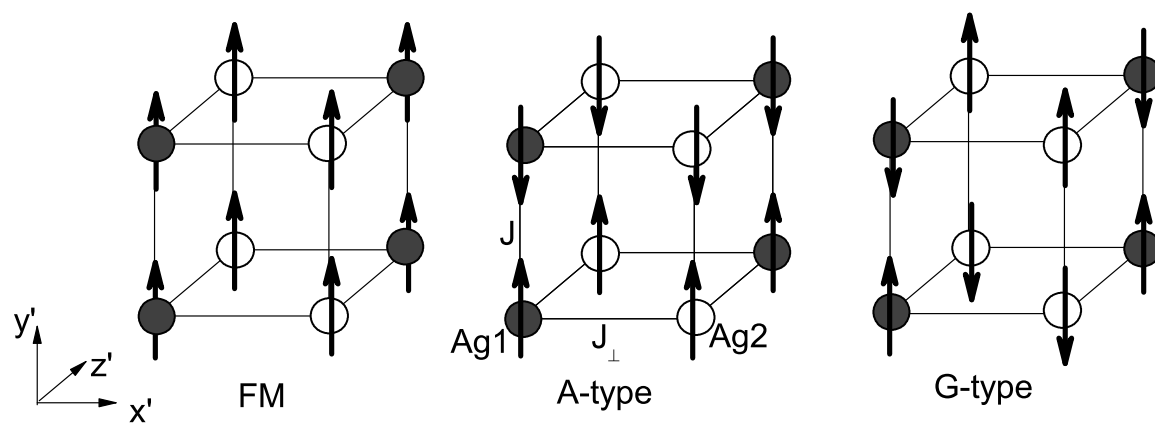
Fig. 1 Zhang.eps

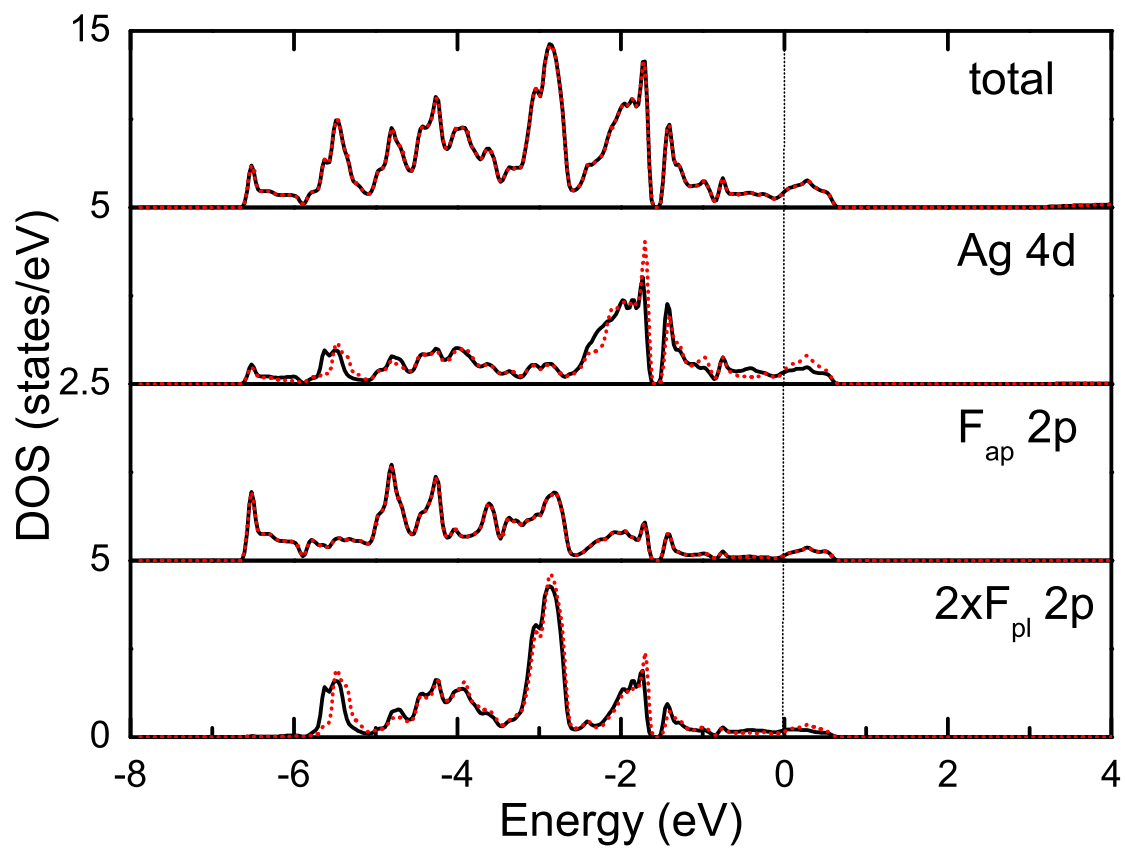
Fig. 2 Zhang.eps

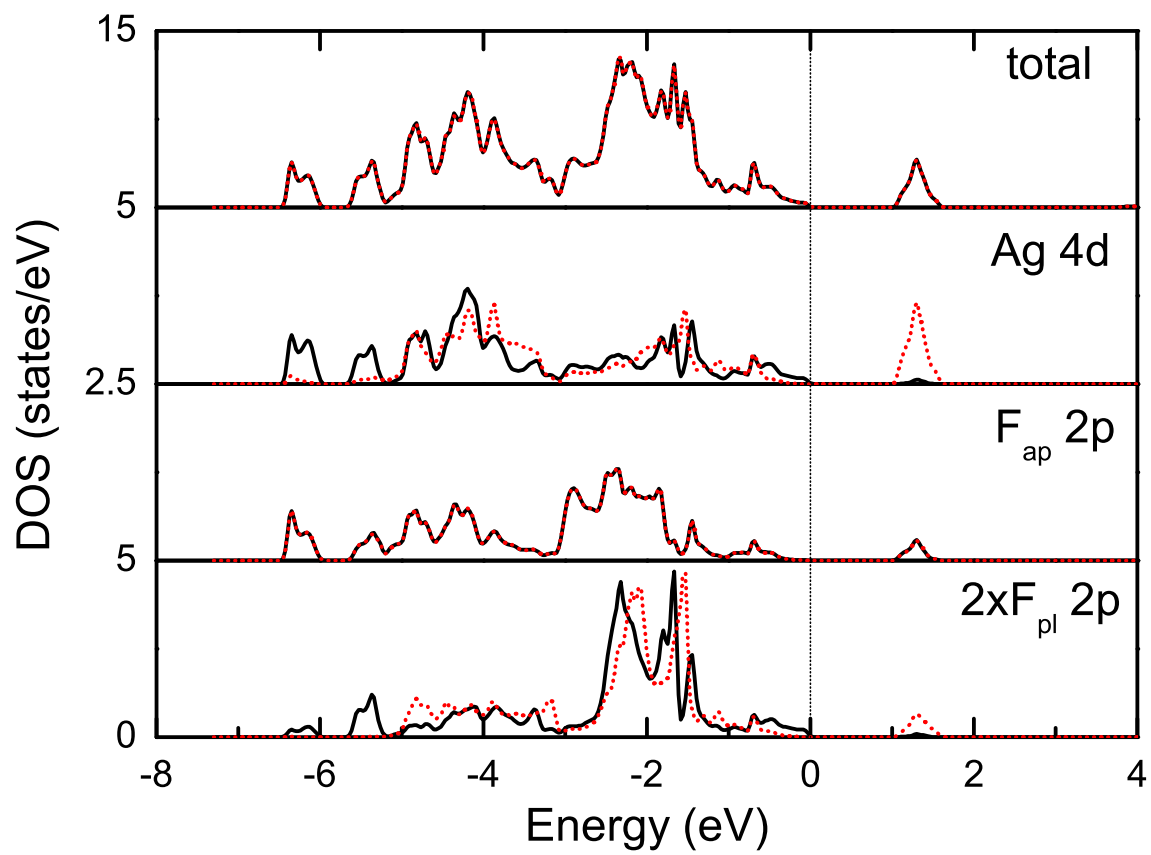
Fig. 3 Zhang.eps

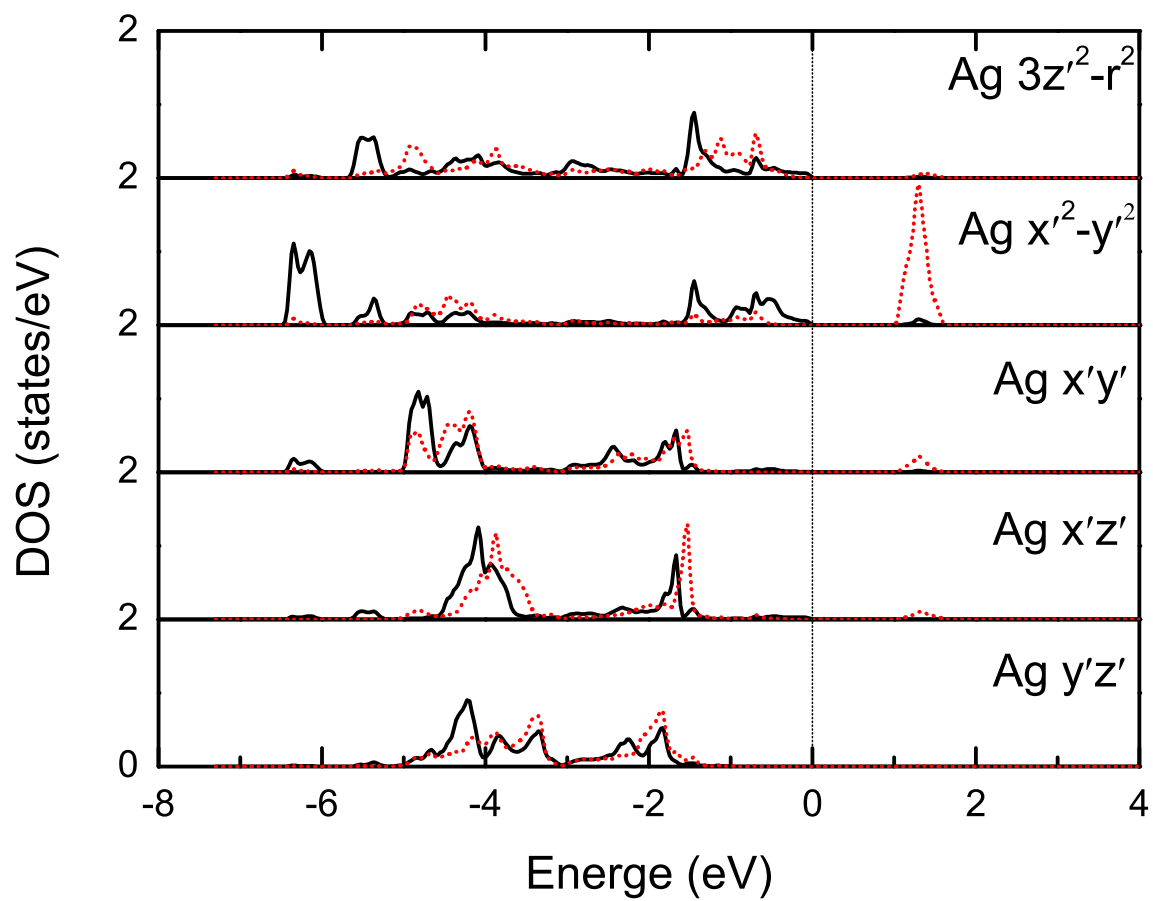
Fig. 4 Zhang.eps

Fig. 5 Zhang.eps

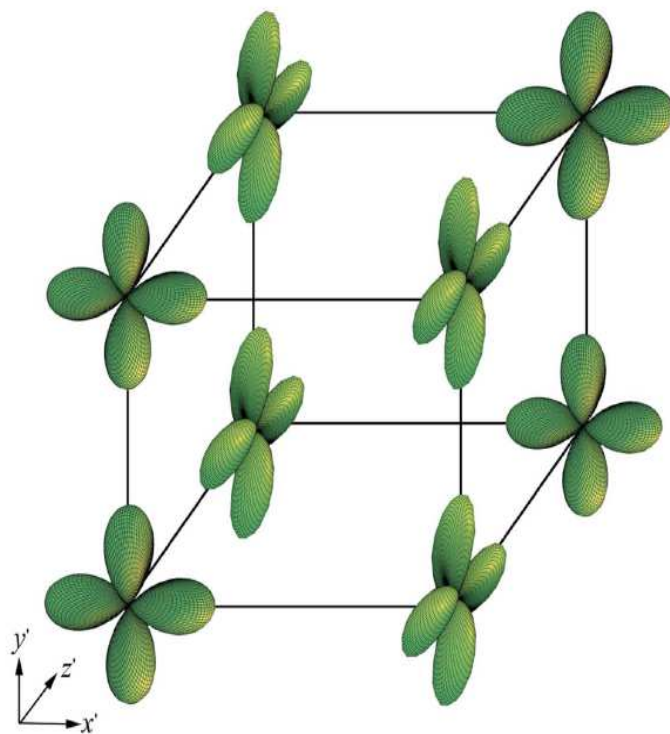
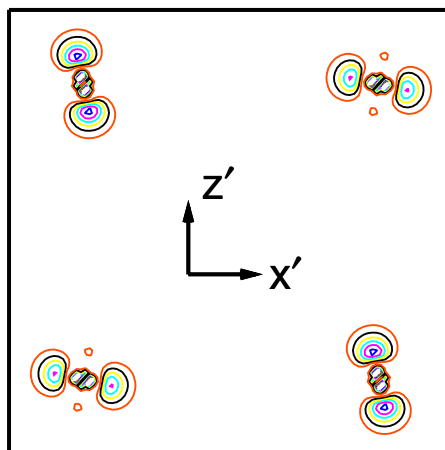
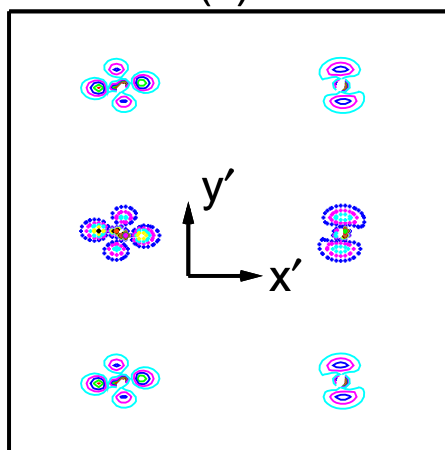
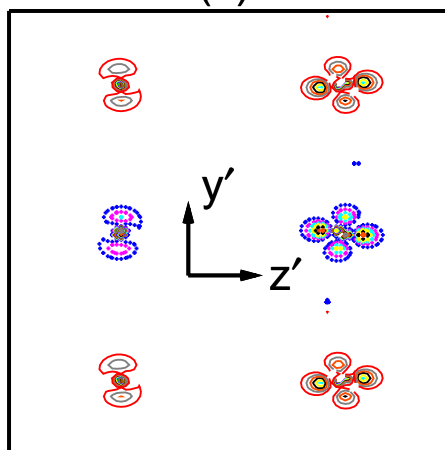


Fig. 6 Zhang.eps

(a)



(b)



(c)